Chin. J. Astron. Astrophys. Vol. 7 (2007), No. 4, 487–495
(*http://www.chjaa.org*)

Chinese Journal of
Astronomy and
Astrophysics

Linear Correlations between Peak Frequency of Gyrosynchrotron Spectrum and Photosphere Magnetic Fields *

Ai-Hua Zhou and Jian-Ping Li

Purple Mountain Observatory, Chinese Academy of Sciences, Nanjing 210008; *zhouah@pmo.ac.cn*

Received 2006 November 18; accepted 2007 April 21

Abstract The gyrosynchrotron spectra are computed in a nonuniform magnetic field case, taking into account the self- and gyroresonance absorption. It is found that the peak frequency ν_p of the gyrosynchrotron spectrum systematically increases with the increasing photosphere magnetic field strength B_0 and increasing viewing angle θ. It is also found for the first time that there are good positive linear correlations between ν_p and B_0, and between $\log \nu_p$ and $\log \theta$, with linear correlation coefficient 0.99 between ν_p and B_0 and 0.95 between $\log \nu_p$ and $\log \theta$. We apply the correlations to analyze two burst events observed with OVSA and find that the evolution tendencies of the photosphere magnetic field strength B_0 estimated from the above expression are comparable with the observational results of *SOHO*/MDI. We also give a comparison of the diagnostic results of coronal magnetic field strength in both uniform and nonuniform source models.

Key words: Sun: flare — sun: radio emission — Sun: magnetic field

1 INTRODUCTION

The coronal magnetic field and its configuration are one of the most important physical quantities in the solar atmosphere and the key to an understanding of the region of solar flares. Microwave (MW) emission during the impulsive phase of a solar flare is generated primarily by the gyrosynchrotron mechanism which involves the interaction of energetic electrons with magnetic fields. Spectroscopy of such emission carries information about the source, such as the magnetic fields and the accelerated electrons. So radio emission is an important tool for the diagnostics of coronal magnetic fields (Bastian, Benz & Gary 1998).

Boischot & Clavelier (1967) using the Razin effect, obtained the result of $B = 0.5\,\mathrm{G}$ for the height where the coronal electron density is $10^7\,\mathrm{cm}^{-3}$. Takakura (1967) found $\nu_p = 3$ or $4\nu_B$ in centimeter wavelength emissions. Guidice & Castelli (1973) noted a tendency for greater correlation at higher peak frequency ν_p for stronger magnetic field strength B_0 at the photosphere.

Several papers (e.g., Batchelor, Benz & Diehl 1984; Gary 1985; Bastian & Gary 1992; Lim, White & Kudu 1992; Zhou et al. 1996) estimated the coronal magnetic field strength B on the basis of simplified relations of Dulk & March (1982) using several additional assumptions. To decrease the number of assumptions, Zhou & Karlisky (1994) presented a more direct diagnostic way to estimate B. Later this method was improved by using a set of more accurate simplified expressions of gyrosynchrotron radiation (Zhou 1998; Zhou et al. 1998; Zhou, Huang & Wang 1999). However, the obtained expressions of the coronal magnetic field strength are based on the uniform source assumption, which may deviate from the reality.

In this paper we compute the gyrosynchrotron spectrum in nonuniform magnetic fields. For simplicity, we assume a magnetic dipole model. We investigate the impact of the photospheric magnetic fields on the gyrosynchrotron spectrum, especially on the peak frequency, because the peak frequency is an important

∗ Supported by the National Natural Science Foundation of China.

spectral parameter that can be quantitatively obtained from high spectral resolution observations of MW bursts. We make linear regression calculations on the correlations between the peak frequency of the gyrosynchrotron spectrum and the photosphere magnetic field strength and between the logarithm of the peak frequency and the viewing angle. We then apply the obtained relationships to an analysis of two observed events of Ovens Valley Solar Array (OVSA) and give the diagnostic results of coronal magnetic strength for the uniform and nonuniform cases.

2 MODEL COMPUTATION AND FIT

According to the general equation of radiative transfer, the flux density is

$$S_{\nu\mp} = \Omega \int_0^{\tau_{\nu\mp}} (\eta_{\nu\mp}/\kappa_{\nu\mp}) e^{-t_{\nu\mp}} dt_{\nu\mp}, \tag{1}$$

where Ω is the solid angle in units of steradian (sr). The subscripts – and + correspond to the X-mode and O- mode, respectively. We consider a power law for the electron energy distribution, $n(E) = GE^{-\delta}$, and an isotropic distribution of the pitch angle. We assume a magnetic dipole field model where the variation of the magnetic field strength with height has the form (Takakura & Scalise 1970)

$$B(h) = B_0 \Big(\frac{d}{d+h}\Big)^3, \tag{2}$$

with B_0 the photosphere magnetic field strength and d the depth of the magnetic dipole below the photosphere. For the magnetic dipole field case we can deduce the flux density of gyrosynchrotron radiation in the quasi-longitudinal propagation case (Zhou, Su & Huang 2004) as

$$S_{\nu\mp} = \frac{G\pi e^2 d}{3c} (2.8 \times 10^6 B_0)^{1/3} \nu^{2/3} \Omega \times 10^{19} \int_{s_0}^{s_m} \varsigma_{s\mp} s^{-2/3} e^{-\tau_{\nu\mp}(s)} ds, \tag{3}$$

where

$$\varsigma_{s\mp} = \frac{1}{2\,|\cos\theta|} \sum_{n>s\sin\theta}^{\infty} \int_{p_0}^{p_m} (a \pm b)^2 (1+p^2)^{-1} (\sqrt{1+p^2} - 1)^{-\delta} dp.$$

In Equation (3), s_0 and s_m are respectively the harmonic numbers of the emission from the lower (h_d) and upper boundary (h_u) of the radio source, p_0 and p_m are the corresponding electron momenta of E_0 and E_m. In the calculation of the optical depth $(\tau_{\nu\mp}(s))$, we consider the combination of the self absorption of the gyrosynchrotron radiation and gyroresonance absorption, $(\tau_{\nu\mp}(s) = \tau^{\rm self}_{\nu\mp}(s) + \tau^{\rm gyro}_{\nu\mp}(s))$, as neither can be ignored in the propagation of the emission in a solar atmosphere with high number density of energetic electrons and high magnetic field strength (Zhou 2005). For the parameters of the burst source, typical values are taken, including $E_0 = 10$ keV, $N = 10^5$ cm^{-3}, and $h_d = 1.8 \times 10^9$ cm.

In this paper we will study mainly the effects of the photosphere magnetic field strength B_0 and the viewing angle θ on the gyrosynchrotron radiation spectrum, so the other parameters are given fixed values. Figures 1 and 2 show the flux density spectra of the gyrosynchrotron radiation for the X-mode and O-mode for a set of values of the photosphere magnetic field strength, B_0. They show that the flux density $S_{\nu\mp}$ and the peak frequency ν_p systematically increase with increasing magnetic field strength B_0. For example, as B_0 increases from 800 to 5000 G, the flux density $S_{\nu\mp}$ at ν=20 GHz increases by about two orders of magnitude and the peak frequency shifts from 3.4 GHz to the higher frequency of 18 GHz.

The flux density spectra for the X-mode and O-mode for four values of the viewing angles θ are given in Figure 3. It shows that the flux densities $S_{\nu\mp}$ and the peak frequencies ν_p for the X-mode and O-mode also systematically increase with increasing viewing angle.

The peak frequency of gyrosynchrotron radiation may be obtained from the above theoretical spectrum (see Figs. 1–3). The accuracy reached in our computed peak frequency is $\pm$ 0.1 GHz . Figures 4 and 5 show the theoretical peak frequency ν_p as functions of the photosphere magnetic field strength B_0 and the viewing angle θ. We can see from Figure 4 that there is a good linear correlation between ν_p (shown for the X-mode) and B_0 in the range $800 \le B_0({\rm G}) \le 5000$, with regression equation,

$$\nu_p({\rm GHz}) = 0.7 + 0.00364 \times B_0({\rm G}) \pm 0.5, \tag{4}$$

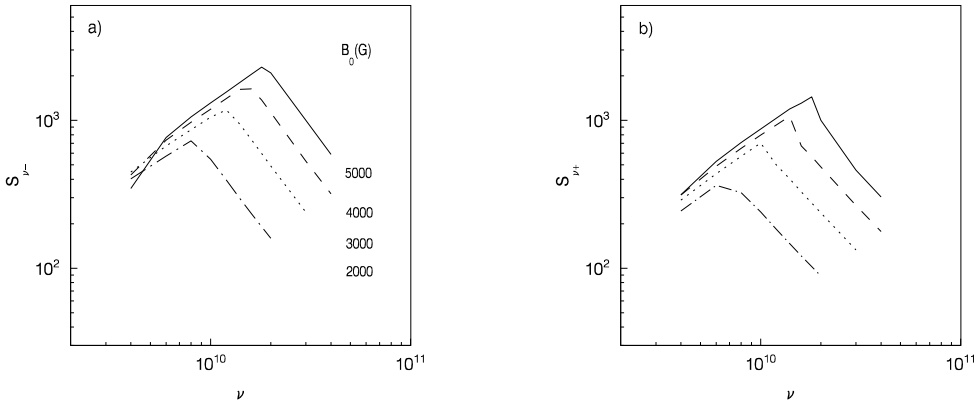

Fig. 1 Flux density ($S_{\nu\mp}$ (sfu)) spectra of gyrosynchrotron radiation for four values of photosphere magnetic field strength, B_0 (G), in the range $2000 \leq B_0(\mathrm{G}) \leq 5000$. Panel (a) for the X-mode, Panel (b) for the O-mode.

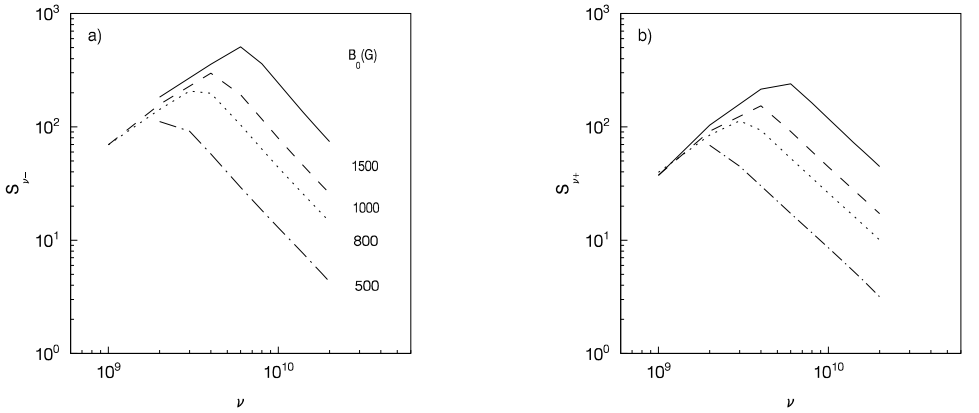

Fig. 2 Same as Fig. 1 but for in the range $500 \leq B_0(\mathrm{G}) \leq 1500$.

and standard error of ν_p $\pm$0.5. The linear correlation coefficient between ν_p and B_0 is 0.99. We note that there is a lower cutoff (0.7 GHz) of ν_p in Equation (4).

Figure 5 shows that there also is a good linear correlation between $\log \nu_p$ (shown for the O-mode) and $\log \theta$ in the range $10^\circ \leq \theta \leq 80^\circ$, with regression equation,

$$\log \nu_p(\mathrm{Hz}) = 9.43 + 0.314 \times \log \theta \pm 0.035, \tag{5}$$

and standard error of $\log \nu_p \pm 0.035$. The linear correlation coefficient between $\log \nu_p$ and $\log \theta$ is 0.95

3 APPLICATIONS

3.1 Observations of Two Events

In this section we will give some applications of the above linear fits in the diagnostics of coronal magnetic field strength. Two burst events are selected. The first event (Event 1) which occurred on 2000 June 3, was an M6.1 flare located in AR9026 (N21E61). The spectral profiles observed by OVSA showed that the peak frequency clearly varied between 8–4 GHz. The second event (Event 2) was in the same active

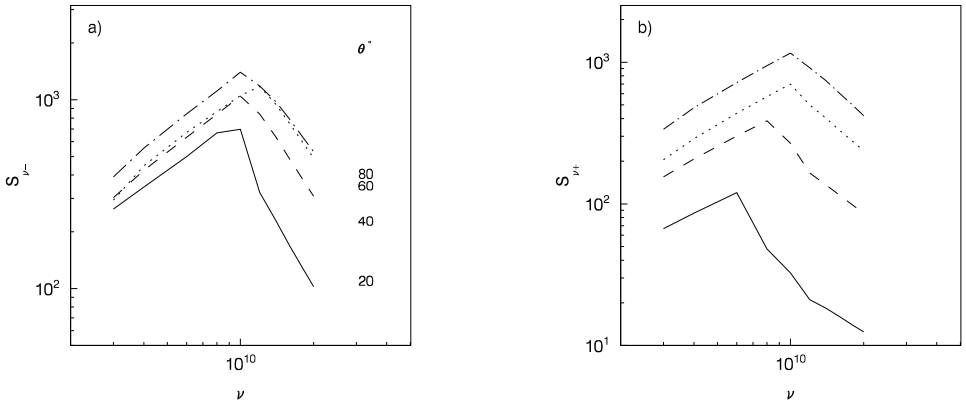

Fig. 3 Same as Fig. 1 but for four different values of the viewing angle, θ.

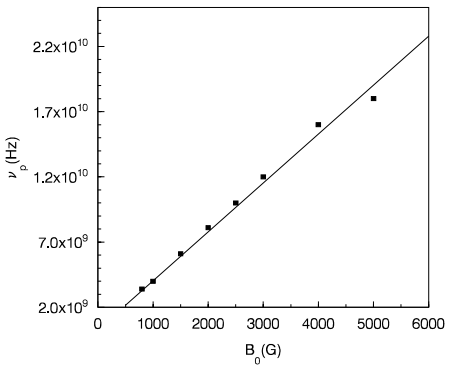

Fig. 4 Linear correlation between ν_p for the X-mode and B_0 in the range $800 \leq B_0(\mathrm{G}) \leq 5000$.

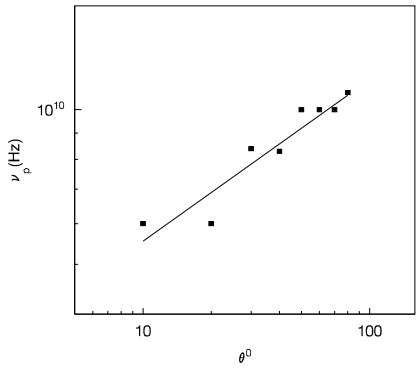

Fig. 5 Linear correlation between $\log \nu_p$ (O-mode) and $\log \theta$ in the range $10^\circ \leq \theta \leq 80^\circ$.

region AR9026 (N22W29), and was an M5.2 flare that occurred on 2000 June 10 . The peak frequency was also evidently varied, but only between 3.2–1.5 GHz. Figures 6 and 7 show the time profiles of Event 1 at 16.4 GHz and of Event 2 at 9.4 GHz along with their associated hard X-ray (HXR) bursts in the M2 channel. The figures show that the MW and HXR burst profiles were very similar for both events, indicating that the MW and HXR emissions could be produced by the same nonthermal electrons.

Figures 8 and 9 show the photosphere magnetic fields observed by *SOHO*/MDI. They are overlaid on the SXR and HXR images observed by *Yohkoh* at the maximum phase. Event 1 was characterized by two footpoint (FP) sources. The upper FP and lower FP corresponded to the positive and negative magnetic field regions, respectively. For Event 2 the emissions of HXR came from a single source. It is located at the lower FP of the flare loop in SXR. In this region the magnetic field was negative (see Fig. 9).

3.2 Evolution of the Photosphere Magnetic Field

Six time instants labelled (t_1–t_6) are selected to study the evolution of the magnetic field strength during the burst. The peak frequencies ν_p and flux densities S_ν observed by OVSA at t_1–t_6 are given in Tables 1 and 2 for the two events, together with the flux S_ν ($\nu = 15$ for Event 1, and 9.4 GHz for Event 2) of the optically thin part.

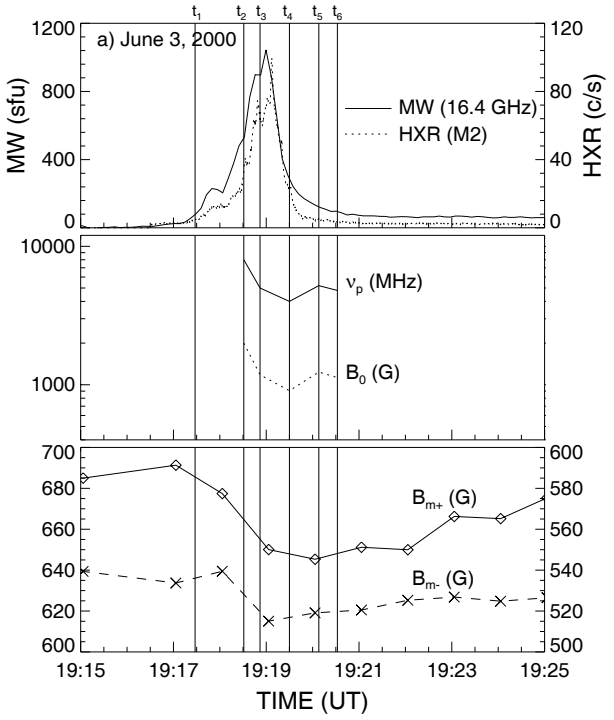

Fig. 6 Time profiles of MW (16.4 GHz) and HXR (M2) bursts of Event 1, observed respectively with OVSA and *Yohkoh*/HXT, peak frequency ν_p (MHz), positive (B_{m+}) and negative (B_{m-} (G)) magnetic field strengths at the photosphere measured by *SOHO*/MDI with high temporal resolution (one minute) and the estimated values of B_0(G) with using Eq. (4) at times t_1–t_6.

For Event 1 the observed peak frequency at t_1 time was 0.5 GHz. At t_2 it increased rapidly to 8 GHz, then it began to decrease until t_4. Then it increased once again from 4 to 5.2 GHz at t_5. After t_5 it continued to decrease. For Event 2 the peak frequency at t_1 was 0.25 GHz. It increased to 3.2 GHz at t_2, then it began to decrease until t_6. The ν_p values of 0.5 and 0.25 GHz are lower than the lower limit of 0.7 GHz, which shows that at early phase of both events the emission may be not gyrosynchrotron radiation.

From the observed peak frequency we can estimate the photosphere magnetic field strength B_0 using Equation (4). The observed peak frequency at t_1 was 0.5 for Events 1, and 0.25 GHz for Event 2, which are below the lower limit of 0.7 GHz, so we cannot estimate the B_0 at t_1. For Event 1 the estimated value of B_0 at t_2 reached 2000 G, then it began to decrease until t_6. For Event 2, B_0 is 686 G at t_2. Then it decreased but increased once again from 275 to 357 G at t_4. After t_4 it continued to decrease. As the peak frequency and photosphere magnetic field strength are linearly correlated, the evolutions of ν_p and B_0 are similar.

We can see from Figures 6 and 7 that the peak frequency of Event 1 was higher than that of Event 2. This agrees with Equations (4) and (5), as Event 1 has a higher photosphere magnetic field strength and a larger viewing angle than Event 2.

The estimated photosphere magnetic field strength B_0 will be compared further with the measured results (B_m) of *SOHO*/MDI for both events. Figure 6 shows, for Event 1, the temporal variations of the measured positive (B_{m+}) and negative (B_{m-}) magnetic field strength. It shows that B_{m+} began to decrease at t_1 till t_4 from about 690 to 648 G. During the decay phase it was nearly constant. The negative magnetic field strength (B_{m-}) also decreased from 535 to 515 G at t_1 to t_4, and after t_4 it was nearly constant also. For Event 2 the emission came only from a single source, which corresponds to a negative magnetic field region (see Fig. 9). Figure 7 shows that the measured photosphere magnetic field strength (B_{m-}) decreased from 168 at t_1 to 150 G at t_4, then it increased again at t_5, which could be measuring error. The temporal

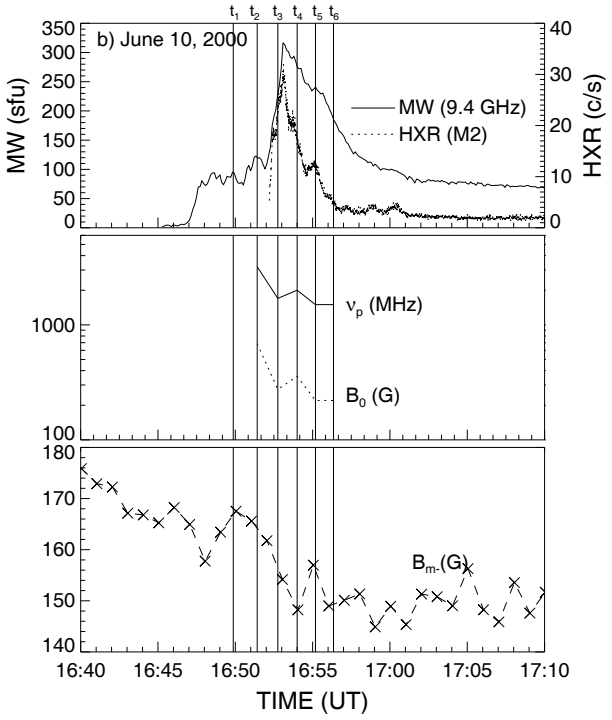

Fig. 7 Same as Fig. 6 except for Event 2.

variations of the measured B_m and the estimated B_0 were rather similar in the two events (see Figs. 6 and 7), which means that the variations of the peak frequency were caused mainly by changes in the magnetic field strength of the burst region in both events.

Figure 10 shows the results of correlation analysis of the observed peak frequency ν_p (GHz) and photosphere magnetic field strength B_m (G). The correlation coefficients, γ, reached 0.89, 0.97 for B_{m+} and B_{m-} for Event 1. For Event 2, it was 0.85. The correlation coefficients are not so good as the theoretical results, due to the small size of the statistical sample and large errors in ν_p (Huang 2006) and B_m, especially for Event 2 (see Fig. 7).

3.3 Diagnostic of Coronal Magnetic Field Strength

3.3.1 Nonuniform Case

Based on Equation (2), the coronal magnetic field strength can be calculated at any height above the photosphere in the nonuniform magnetic dipole field model. The calculated coronal magnetic field strength at the height of 3.2×10^9 cm above the photosphere, B_h, is given for the selected times t_2–t_6 for the case of the magnetic dipole, with d=3.5×10^9 in Tables 1 and 2 and shown in Figure 11.

3.3.2 Uniform Case

The magnetic field strength in the uniform source case is also calculated for comparison with the results in nonuniform source case. The magnetic field strength, B_u, in the uniform case, is (Zhou & Karlisky 1994),

$$B_u = \left[\frac{2\Omega\nu^2}{S_\nu A_1}\nu_p^{1.3+0.98\delta}\nu^{-0.78-0.9\delta}(2.8\times10^6)^{-2.52-0.08\delta}\right]^{\frac{1}{0.52+0.08\delta}}, \quad (6)$$

where $A_1 = 4.24\times10^{14+0.3\delta}\sin\theta^{0.34+0.07\delta}$.

The viewing angle is 61° for Event 1 and 29° for Event 2. The values of B_u can be calculated, taking $\Omega = 1.3\times10^9$, for a set of known parameters: δ, ν_p, θ, and fixed frequencies (15 GHz for Event 1 and

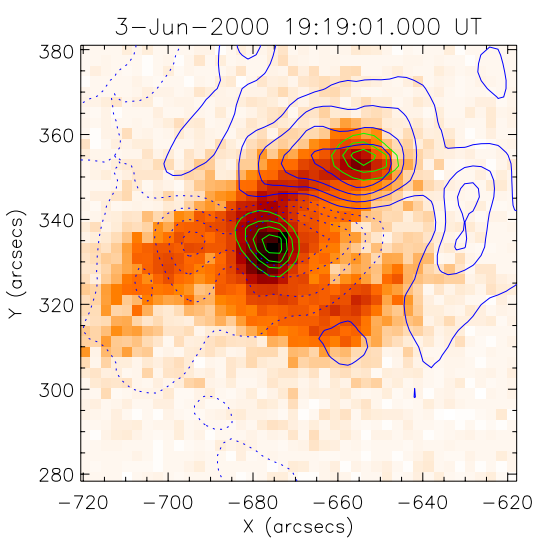

Fig. 8 Photospheric magnetic fields measured by *SOHO*/MDI (blue contours at ±100, 300, 500 and 700), overload on the HXR (green contours) and SXR images (red contours) observed by *Yohkoh* at the maximum phase of Event 1.

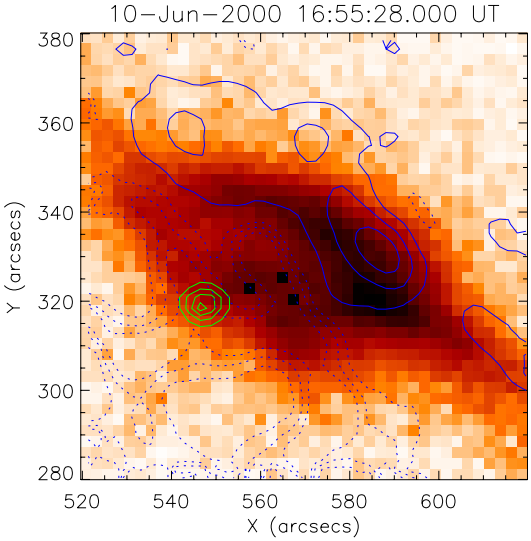

Fig. 9 As Fig. 8 but for Event 2. Contours at (100, 300, 500) and (–150, –100, –50).

Table 1 Observed Spectral Parameters and Calculated Magnetic Field Strengths at Selected Times of Event 1

	t_1	t_2	t_3	t_4	t_5	t_6
S_{15G} (sfu)	20	160	360	112	50	40
δ		4.5	2.8	3.2	4.5	4.0
ν_p (GHz)	0.5	8.0	5.0	4.0	5.2	4.8
B_0 (G)		2000	1180	906	1236	1126
B_h (G)		286	168	129	176	160
B_u (G)		608	197	114	144	56

Table 2 Observed Spectral Parameters and Calculated Magnetic Field Strengths at Selected Times of Event 2

	t_1	t_2	t_3	t_4	t_5	t_6
$S_{9.4G}$ (sfu)	80	110	240	265	220	175
δ		4.5	4.0	2.8	4.0	4.0
ν_p (GHz)	0.25	3.2	1.7	2.0	1.5	1.5
B_0 (G)		686	275	357	220	220
B_h (G)		98	39	51	31	31
B_u (G)		54	43	33	22	26

9.4 GHz for Event 2). See Tables 1 and 2 and Figure 11. We see that B_u in the uniform case is comparable to B_h at the height of 3.2×10^9 cm in the nonuniform case as regards both size and variation for both Events 1 and 2. The time evolution of both B_u and B_h is similar to that of the B_m observed by *SOHO*/MDI, i.e., a decrease in the rise phase, then nearly constant during the decay phase.

4 CONCLUSIONS

In this paper gyrosynchrotron spectra for quasi-longitudinal propagation are computed for the case of magnetic dipole, using the general equation of radiative transfer and taking into account the self absorption and gyroresonance absorption. It is emphasized that these spectra are general. It is found that the peak frequency ν_p of the calculated spectrum systematically increases with increasing photosphere magnetic field strength, B_0, and increasing viewing angle θ. Good and positive linear correlations exit between ν_p and B_0 and between $\log \nu_p$ and $\log \theta$, with respective correlation coefficients 0.99 and 0.95 and respective standard errors 5% and 8%.

We have carried out correlation analysis between the observed peak frequency ν_p and photosphere magnetic field strength B_m for two events. For Event 1 the correlation coefficient reached 0.89, 0.97 for B_{m+} and B_{m-}. For Event 2, it was 0.85. The positive correlation between ν_p and B_0 we found and that found by Guidice and Castelli are in agreement with our theoretical correlation result (see Eq. (4)).

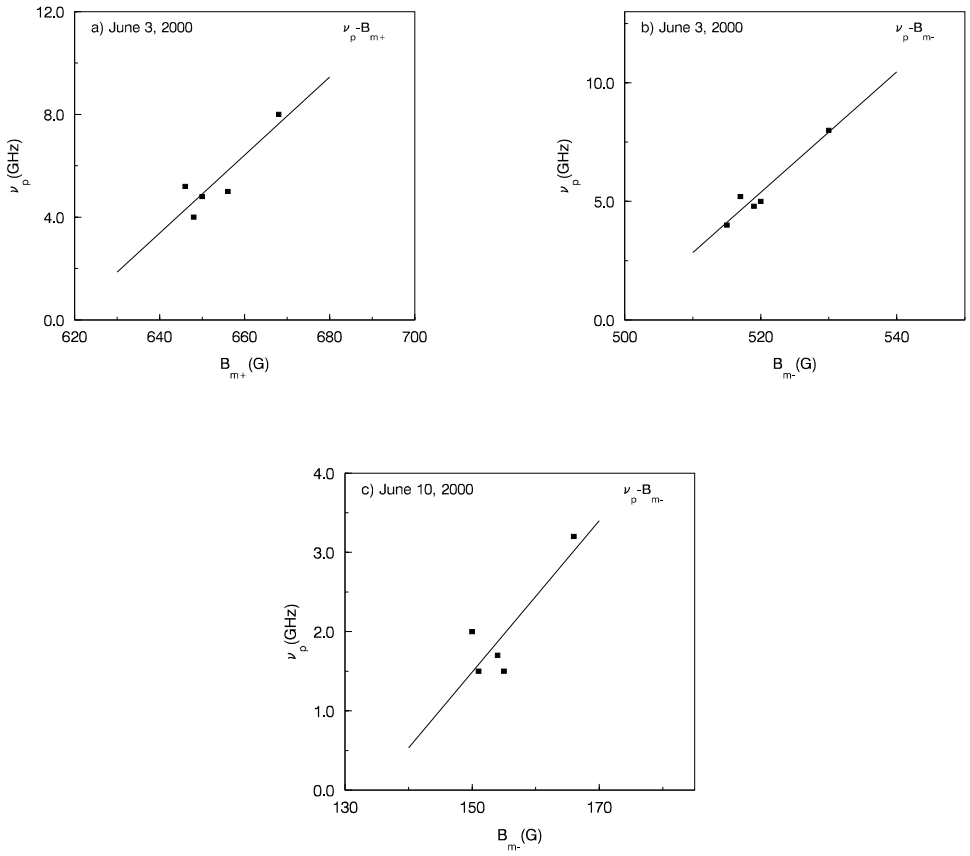

Fig. 10 Correlation cases between the observed peak frequency ν_p (GHz) and the measured photosphere magnetic field strength B_m (G), where (a) and (b) are for Event 1 and (c) for Event 2, respectively.

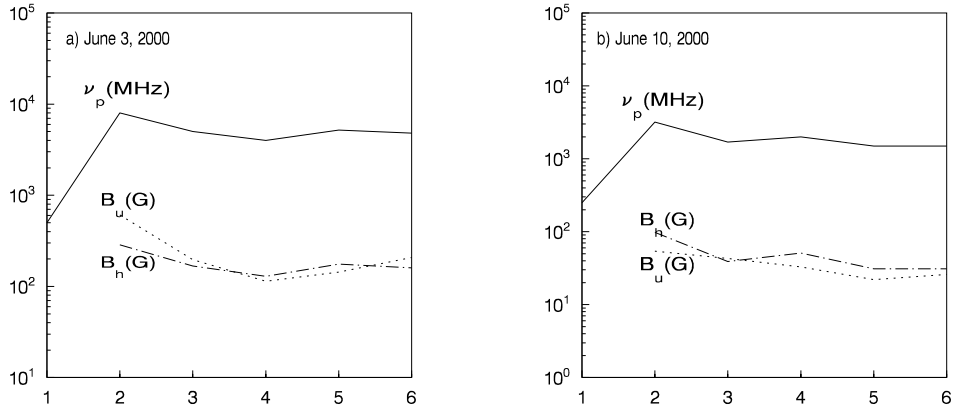

Fig. 11 Observed peak frequency ν_p (MHz) with OVSA, and calculated coronal magnetic field strength at height 3.2×10^9 cm, B_h (G) in the nonunuform case and B_u (G) in the uniform case at times t_1–t_6. Panel (a) for Event 1, Panel (b), for Event 2.

Using the linear relation between ν_p and B_0 (Eq. (4)), the photosphere field strength, B_0, can be estimated from the observed peak frequency ν_p. It is found that the temporal evolutions of the estimated photosphere field strength, B_0 and the measured one, B_m behaved similarly during Events 1 and 2, which means that the variations in the peak frequency were caused mainly by changes in the magnetic field strength in both events. We also note, however, that the absolute values of photospheric magnetic field strength B_0 and B_m and their variation amplitudes were different. The values of B_0 and its variation amplitude were larger than the measured results of B_m. This might have been caused by a more elevated lower boundary (h_d) of 1.8×10^9 cm of the burst source. If h_d is taken as 6×10^8 cm above the photosphere, the estimated B_0 and its variation will be close to the measured results of B_m. Note that we adopted the magnetic dipole field model only for simplicity, and it could well deviate from reality. On the other hand, a fairly strong energetic electron beam might diminish the measured photosphere magnetic field strength (Ding, Qui & Wang 2002).

We calculated both the coronal magnetic field strength in the uniform case (B_u) and in the nonuniform case (B_h). We find that B_u is comparable to B_h at height 3.2×10^9 cm regarding both time variation and magnitude during the flares of Events 1 and 2. B_u and B_h also evolved similarly to the B_m observed by *SOHO*/MDI, i.e., a decrease in the rise phase, then nearly constant during the decay phase.

Acknowledgements This study is supported by the NSFC grant Nos. 10273025 and 10333030. The authors thank Prof. G. L. Huang, Q. Fu and Mr. X.D. Wang for helpful discussions.

References

Bastian T. S., Gary D. E., 1992, Solar Phys., 139, 357
Bastian T. S., Benz A. O., Gary D. E., 1998, Ann. Rev. Astron. Astrophys., 36, 131
Batchelor D. A., Benz A. O., Wiehl H. J., 1984, ApJ, 280, 879
Boischot A. Clavelier B., 1967, Astrophysical Letters, 1, 7
Ding M. D., Qui J., Wang M., 2002, ApJ, 576, L83
Dulk G. A., Marsh K. A., 1982, ApJ, 259, 350
Gary D. E., 1985, ApJ, 297, 799
Guidice D. A., Castelli J. P., 1973, in R. Ramaty, R. G. Stone eds., a Symposium, Greenbelt, Md., Sept. 28-30, High Energy Phenomena on the Sun, p.87
Huang G. L., 2006, Chin. J. Astron. Astrophys. (ChJAA), 6, 113
Lim J., White S. M., Kundu M. R. et al., 1992, Solar Phys., 140, 343
Takakura T., 1967, Solar Phys., 1, 304
Takakura T. Scalise E. Jr., 1970, Solar Phys., 11, 434
Zhou A.-H., 1998, Chin. Sci. Bull., 43, 1183
Zhou A.-H., 2005, Chin. Astron. Astrophys., 29, 243
Zhou A.-H., Karlisky M., 1994, Solar Phys., 153, 441
Zhou A.-H., Huang G.-L., Wang X.-D., 1999, Solar Phys., 189, 345
Zhou A.-H., Su Y.-H., Huang G.-L., 2004, Chin. Phys. Lett., 21, 2067
Zhou A.-H., Fu Q., Zhang H. Q. et al., 1996, Acta Astron. Sin., 37, 212
Zhou A.-H., Ma C.-Y., Zhang J. et al., 1998, Solar Phys., 177, 427